AIAA Journal
Vol. 39, No. 10, October 2001

Novel Design of a Bonded Lap Joint

Qing-Gang Zeng* and C. T. Sun†
Purdue University, West Lafayette, Indiana 47907-1282

A new design of a single-lap joint was proposed and investigated experimentally. In this new design, load eccentricity as well as singular peel stresses in the joint interface were avoided. In fact, numerical calculations show that, in the new design, the peel stress becomes compressive in the joint end region, and the shear load is more evenly transferred over the length of the joint. Two adherend layups, that is, $[0/90/0/90]_{2s}$ and $[90/0/90/0]_{2s}$, were considered. Experimental results show that the strength of the new joint is significantly higher than that of the conventional single-lap joint. It is believed that even higher strength can be obtained by optimizing the new design configuration.

Introduction

MANY structures consist of a number of basic parts that are connected together to take up the load. The connections or joints are usually the weakest locations in the structure. Among the many technical challenges facing engineers using advanced composite materials is joining composite parts or composite to metallic components. Even though the use of composite materials can greatly reduce the number of parts, joining parts is still unavoidable. Traditional joining methods for metals such as welding and soldering are apparently unsuitable for fiber-reinforced composites. Compared to mechanical fastening, adhesive bonding is attractive for joining fiber-reinforced composite structures because it reduces the localized stresses encountered when using bolts and rivets. Moreover, bolts and rivets cut the continuous reinforcing fibers, and, as a result, may greatly reduce the overall load carrying capacity of the structure.

Adhesively bonded joints are used in many different configurations, among which the most commonly used are single-lap joints, double-lap joints, scarf joints, and step-lap joints.[1–3] The single-lap joint is generally the simplest and least expensive of all joints to manufacture. However, because of its intrinsic load eccentricity and the abrupt change of load path, both the normal (peel) and shear stresses are highly localized at the two joint ends; thus, the conventional lap joints are not efficient in load transfer.[4] Moreover, because the interfacial normal stress is tensile and theoretically singular at the joint ends, it can initiate failure at these locations. Although tapering the adherend or adding adhesive fillets at joint ends can lead to some reduction of peel stresses in the lap joint, these improvements are, however, quite modest.[5,6]

Structural adhesives have relatively poor resistance to peel or cleavage stresses. Therefore, an obvious step to improve joint strength is to reduce the magnitude of peel stress or to make it compressive. To obtain maximum joint efficiency, the interfacial shear stress distributions should also be made more uniform.

In this paper, a new wavy bonded lap joint is proposed and investigated. With this new joint design, the interfacial normal stress is compressive at the two joint ends, and the interfacial shear stress distribution is less localized. Experimental results show that the wavy joint has much greater strength than the conventional lap joint.

Conventional Single-Lap and New Wavy-Lap Designs

For comparison, a two-dimensional sketch of the conventional single-lap joint is shown in Fig. 1. Only the case of identical adherends is considered in this study. The length of both outer adherends is L, the overlap (joint) length is l, and the thickness of adherend and adhesive are t_a and t_g, respectively.

The general shape of the new wavy joint is first laid out as shown in Fig. 2. It is seen that the joint is an assemblage of straight segments, and the global load eccentricity is avoided. Subsequently, we choose the waviness angles (Fig. 2) $\alpha = \beta = \tan^{-1}(2t_a/l')$ and round out sharp corners of the joint with an adequate radius R. The final joint shape selected is shown in Fig. 3. The shape chosen here is mainly for simplicity; other possible shapes may be as effective.

Strictly speaking, the two adherends in this wavy joint are not in a collinear configuration. The dashed lines in Fig. 2 show this. If a collinear configuration is desired, then the thickness of the adhesive must be taken into account during the first design step. Because the thickness of the adhesive is very small compared with that of the adherends in this study, it is neglected during the design process.

The values of the geometrical parameters for both conventional and wavy joints are given in Table 1. Even though $l' < l$, the overall bonding areas are the same for the two joints. This ensures that analysis and test results of these joints can be directly compared. The only dimension that is not shown in the Figs. 1 and 2 is the width of specimen, which is $d = 25.4$ mm. The material for adherends is AS4/3501-6 carbon/epoxy. Two different layups, $[90/0/90/0]_{2s}$ and $[0/90/0/90]_{2s}$, are used. The 0-deg direction is parallel to the longitudinal (loading) direction of the joint. The reason for choosing these two layups is to study the difference between 90–90 deg and 0–0 deg bonding interfaces. The material constants of AS4/3501-6 are listed in Table 2. The two adherends are bonded together with a layer of film adhesive FM73M, which is treated as an isotropic material. The elastic constants for FM73M are also listed in Table 2.

Experimental Studies

The fabrication of conventional single-lap joints is as follows. First a 30×30 cm, 16-ply flat composite panel of the desired layup sequence was fabricated using an autoclave following the standard curing cycle. After curing, the panel was cut by a water jet into two pieces with the desired dimensions. The bonding areas were first wiped with a clean methyl ethyl ketone (MEK) solvent dampened nonlinting paper wiper; then it was abraded with 320 grit silicon carbide abrasive papers until no evidence of surface gloss was visible. Finally, it was wiped with a clean dry cloth to remove particles from sanding followed by repeatedly wiping with MEK solvent dampened paper wipers until no further indication of residue was visible on the paper. After drying these adherends for 30 min, an FM73M film adhesive (nominal thickness of 0.13 mm) was placed between the bonding surfaces of the parts. Alignment tabs (see Fig. 1), which were made of the same adherend material and layups, were also bonded to the adherends with FM73M film adhesive. After assembly of the details, the part was cured in the autoclave at 121°C (250°F) under the manufacturer's recommended pressure of 0.28 MPa (40 psi) for 1 h. Finally, the assembly was cut by a water jet into desired joint dimensions. To protect the specimen from local damage caused by gripping of the testing machine, 2.54×2.54 cm end tabs made of copper clad laminate (printed circuit board) were used.

Received 10 June 2000; revision received 11 March 2001; accepted for publication 10 April 2001.

*Graduate Student, School of Aeronautics and Astronautics.
†Neil Armstrong Distinguished Professor, Aeronautical and Astronautical Engineering, School of Aeronautics and Astronautics. Fellow AIAA.

For the wavy joint, two special caul plates with the desired wavy surface were needed to form the special wavy shape for the composite adherends. At first the two special wavy caul plates were used to cure the wavy-shaped composite panel. Then they were used as supports during the bonding cure cycle. Apart from these, the wavy specimen preparation procedure is the same as that for the flat joint. No additional work is needed except for the two wavy forming plates. Excessive adhesive was carefully removed by a razor blade after bonding. Extreme care was taken to avoid damage to the composite and to ensure a clean right angle at the joint ends. Figure 4 shows the top and side views of the wavy-lap joint.

All specimens were tested using an 89-kN servohydraulic MTS testing machine at room temperature. The crosshead-loading rate was 0.001 mm/s. For each lay-up, specimens tested for the flat single-lap joint and the wavy-lap joint were in two and three groups, respectively. The specimens in each group were made from the same composite panel and were bonded at the same time. For the flat single-lap joint, one group consisted of 10 specimens, whereas for the wavy-lap joint, one group consisted of 5 specimens. Figure 5 shows typical load displacement curves for the four different kinds of specimen. The most important results are that the wavy joints are much stronger than the conventional joints for both types of adherends and that the wavy joint appears to have the same stiffness as the conventional joint.

The onset of failure during the experiments was monitored in situ using a microscope, and failed specimens were inspected using a high-power microscope. We managed to catch the failure initiation of all of the single-lap joint specimens and the wavy joint with $[0/90/0/90]_{2s}$ adherends. The wavy joint specimens with $[90/0/90/0]_{2s}$ adherends failed suddenly. In this case, the location of failure initiation was estimated by interpreting the failed specimen and was confirmed by analysis.

For the $[90/0/90/0]_{2s}$ adherend, the peak loads for both joints are listed in Table 3. For the single-lap joints, the average peak load is 4.06 kN. For the wavy-lap joints, all specimens show a significant increase in strength. The average peak load is about 2.2 times that of the conventional single-lap joints.

The failure of the flat single-lap joint that initiated at the edge of the joint is likely due to the highly localized interfacial stresses. Matrix cracking occurred in the 90-deg layers adjacent to the bonding interface at both ends of the joint (see Fig. 6). The matrix crack

Table 1 Joint geometrical parameters

Dimension	Value
Length of outer adherends L, mm (in.)	101.6 (4)
Horizontal length of wavy overlap l', mm (in.)	25.4 (1)
Length of flat overlap l, mm (in.)	27.94 (1.1)
Thickness of adherends t_a, mm (in.)	2.0 (0.08)
Thickness of adhesive t_g, mm (in.)	0.127 (0.005)
Fillet radius for wavy joint R, mm (in.)	10.16 (0.4)

Table 2 Elastic properties of joint materials

Material	Constants
AS4/3501-6	$E_1 = 148$ GPa, $E_2 = E_3 = 10.5$ GPa, $G_{12} = G_{13} = 5.61$ GPa, $G_{23} = 3.17$ GPa, $\nu_{12} = \nu_{13} = 0.3$, $\nu_{23} = 0.59$
FM73M	$E_g = 2.2$ GPa, $\nu_g = 0.31$

Table 3 Test results of $[90/0/90/0]_{2s}$ single-lap and wavy-lap joints

	Average, kN			
Joint	Group 1	Group 2	Group 3	Total
Single lap	3.94	4.07	NA	4.04
Wavy lap	9.46	7.87	8.82	8.65

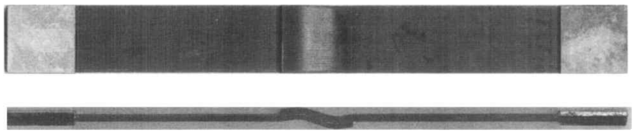

Fig. 4 Top and side views of the wavy-lap joint specimen.

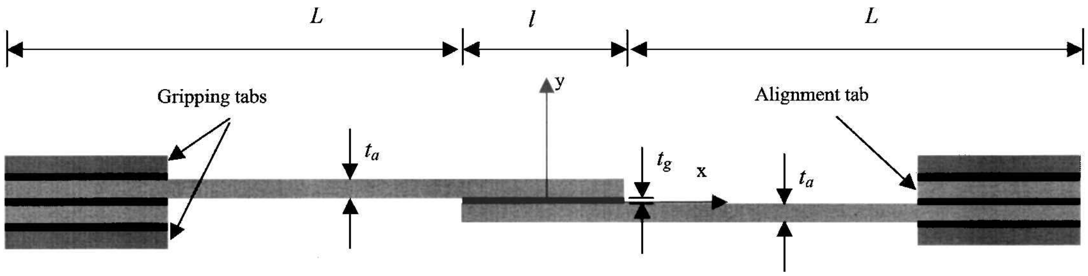

Fig. 1 Geometry and dimensions of a single-lap joint.

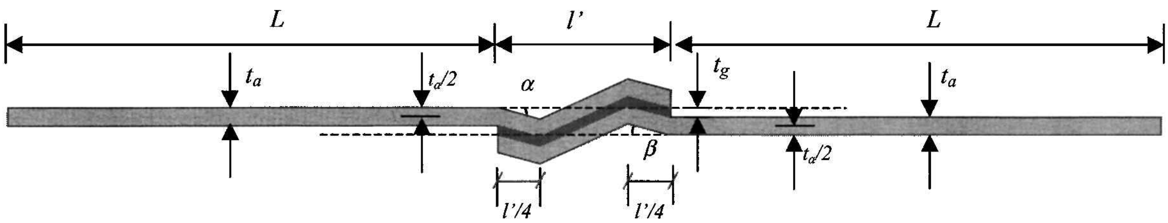

Fig. 2 Geometry of the preliminary design of wavy joint.

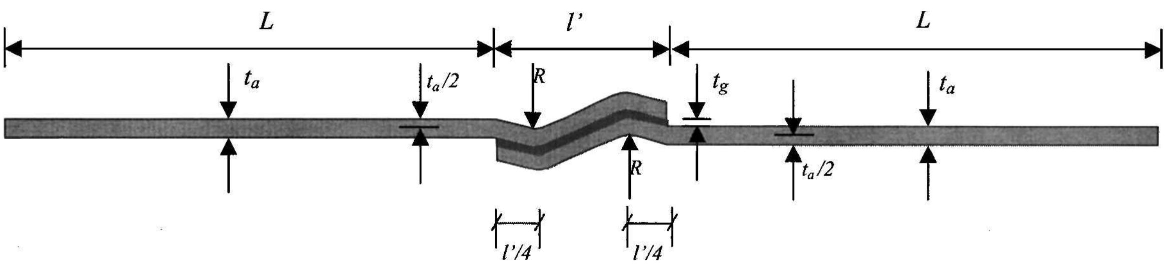

Fig. 3 Geometry and dimensions of the wavy-lap joint.

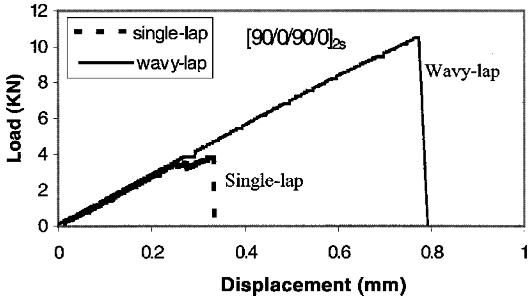

a) $[90/0/90/0]_{2s}$

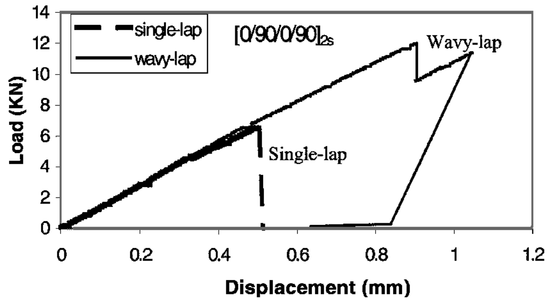

b) $[0/90/0/90]_{2s}$

Fig. 5 Typical load-displacement curves.

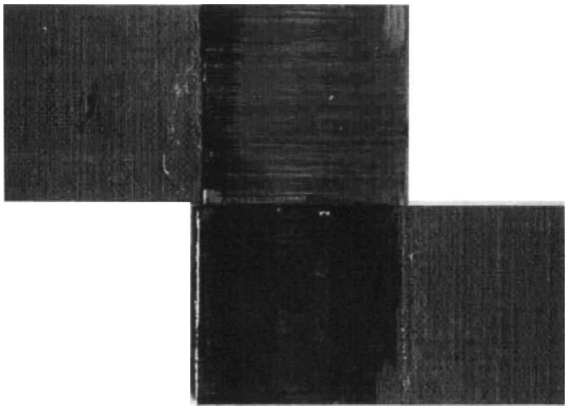

a) Top view

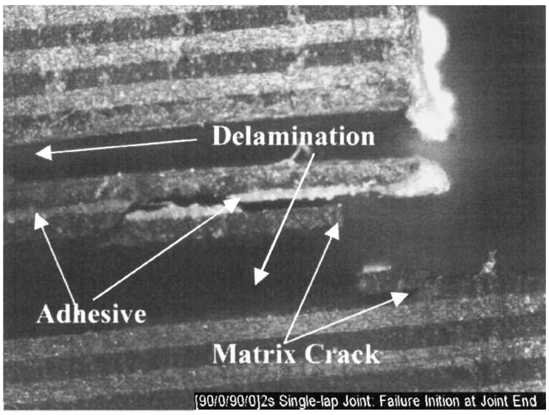

b) Side view

Fig. 6 Typical failure mode in the $[90/0/90/0]_{2s}$ single-lap joints.

led to delamination between the cracked 90-deg layer and the adjacent 0-deg layer. The extension of this delamination crack caused final failure of the joint. This delamination process corresponds to the sudden load drop in the load displacement curve. Failure in the wavy joint was also triggered by matrix cracking in the 90-deg layers bonded to the adhesive layer. Subsequent delamination along the 90/0 deg interfaces led to the final failure. However, the failure initiation location was not at the joint edges; it took place inside the curved region of the joint (Fig. 7).

Table 4 Test results of $[0/90/0/90]_{2s}$ single-lap and wavy-lap joint

	Average, kN			
Joint	Group 1	Group 2	Group 3	Total
Single lap	6.56	6.25	NA	6.34
Wavy lap	10.83	10.04	9.10	9.86

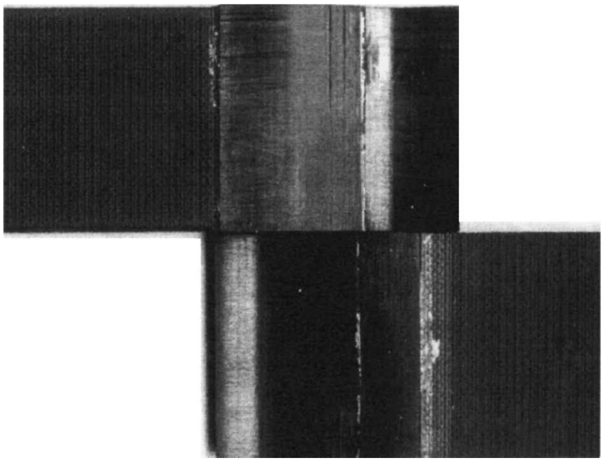

a) Top view

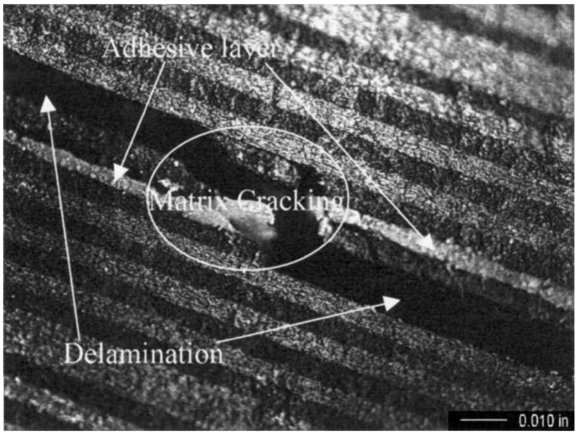

b) Side view

Fig. 7 Typical failure mode in the $[90/0/90/0]_{2s}$ wavy-lap joint.

For conventional and wavy joints with $[0/90/0/90]_{2s}$ adherends, test results are given in Table 4. Note that these joints yielded higher strengths than the respective joints with $[90/0/90/0]_{2s}$ adherends. The average strength of the wavy joint is more than 1.5 times the average strength of the conventional joint.

Failure modes in these two types of joints with $[0/90/0/90]_{2s}$ adherends are quite different. Failure in the flat single-lap joint is in the form of cohesive failure, that is, fracture of the adhesive layer, which initiated at both edges of the joint. No damage in composite adherends was observed. For the wavy-lap joint, failure occurred in the two adjacent 90-deg layers at the midplane of the laminate in the curved joint region. The matrix crack led to the first delamination along the adjacent 90/0 deg interface, resulting in a sudden load drop. On increasing the load, another matrix cracking took place inside the 90-deg layer that is right next to the 0-deg layer adjacent to the bonding interface. This matrix crack led to another delamination that caused the final joint failure. Figures 8 and 9 show the failed conventional single-lap and the wavy-lap specimens, respectively.

For comparisons, all test data are summarized and presented in Fig. 10. The data point indicates the average value of each group.

Analysis of Interfacial Stresses

Analyses of conventional single-lap joints, loaded in tension have been performed by many authors.[4,7] Researchers are still trying to improve analytical solutions that are more efficient in identifying

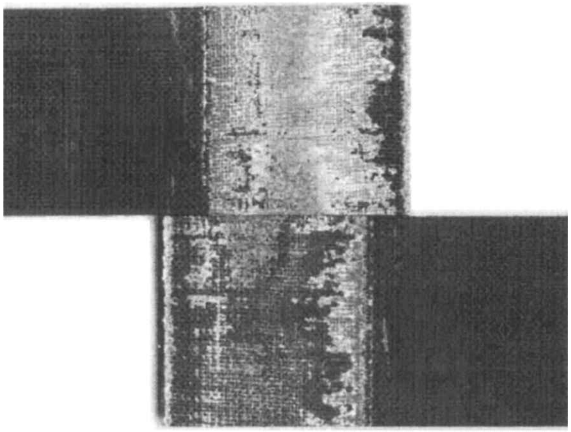

a) Top view

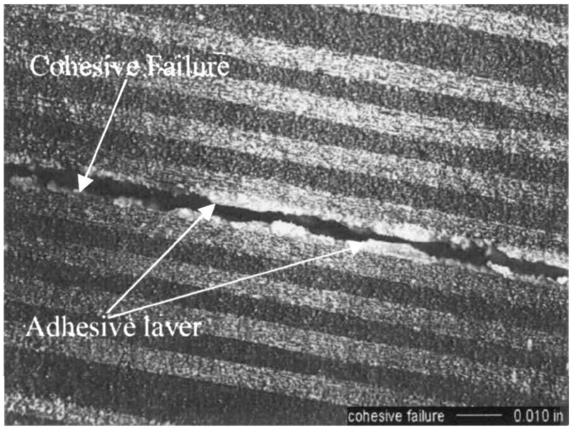

b) Side view

Fig. 8 Typical failure mode in the $[0/90/0/90]_{2s}$ single-lap joint.

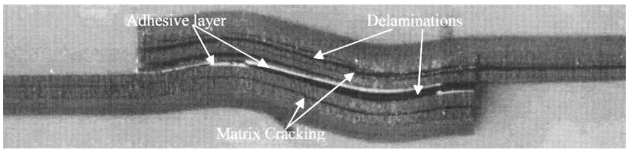

Fig. 9 Typical failure mode in the $[0/90/0/90]_{2s}$ wavy-lap joint (side view).

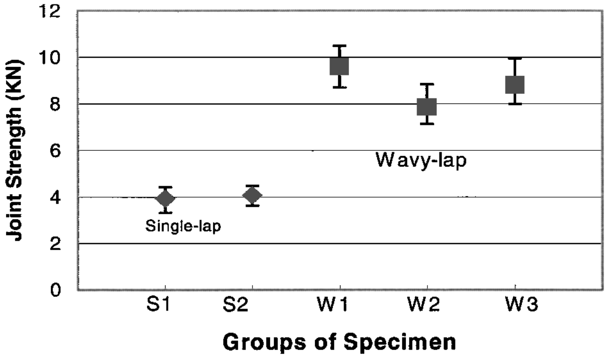

a) $[90/0/90/0]_{2s}$

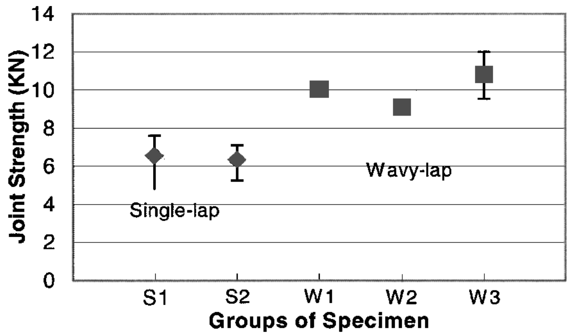

b) $[0/90/0/90]_{2s}$

Fig. 10 Comparison of strengths of conventional and wavy lap joints.

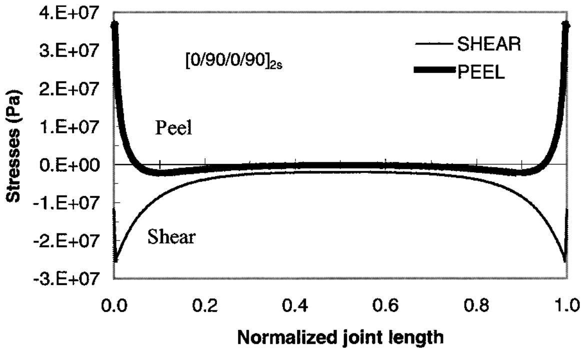

a) $[90/0/90/0]_{2s}$

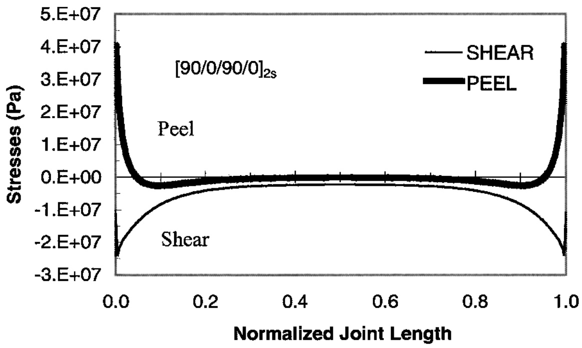

b) $[0/90/0/90]_{2s}$

Fig. 11 Interfacial stress distributions in single-lap joints at a tensile load of 3.6 kN.

key parameters for design.[8] Because of the complex shape of the new wavy joint, analytical solutions are not readily available. We resort to the finite element method for interfacial stress analyses of both types of joint. Even though the adhesive may yield at some highly localized stress concentration region, it remains within the elastic limit in the joint region. Thus, the adherends and adhesive are considered to be elastic in the analysis of interfacial stresses.

Geometrically nonlinear two-dimensional analyses are performed using the commercial code ABAQUS.[9] Geometric boundary conditions include clamping at one end and sliding at the other. The edge nodes at the sliding side are constrained to have the same horizontal displacement. A distributed force is applied horizontally at the sliding end. Plane strain elements CPE4 are used for both adherend and adhesive. Each lamina of the composite adherend is modeled by one element in the thickness direction except for the lamina adjacent to the adhesive layer, which is subdivided into four elements to obtain more accurate interfacial stresses. Thus, a total of 19 elements are used across the thickness of one adherend. For the adherends outside the joint region, 200 elements with a bias factor of 0.46 are employed. Six elements across the thickness of the adhesive layer are used. In an effort to recover traction-free boundary conditions at the joint edges, a very fine mesh (500 elements) is used along the overlap length of the joint. Thus, a total of 29,600 elements are used in this model. Stresses calculated along the centerline of the adhesive are regarded as the average interfacial stress values over the thickness of the bond line. To account for the varying fiber orientation of the wavy joint and possible large deflections/rotations of the joints, the ORIENTATION parameter provided by ABAQUS is employed. Thus, the material properties of each element vary with the rotation and deformation of each element.

For the analysis of the conventional single-lap joint, a total tensile force of 3.6 kN is applied. For the wavy lap joint, the applied tensile load is 12.0 kN. The interfacial stress distributions for both types of joints are shown in Figs. 11 and 12, respectively. The stresses shown in Fig. 12 are normal and shear stresses with respect to the curved bonding interface. It is evident that the adherend stacking sequence does not have any appreciable influence on the distribution of interfacial stresses. However, there are substantial differences between the new and conventional joints.

The well-known characteristics of interfacial stresses in the conventional single-lap joint are clearly shown in Fig. 11. Both interfacial normal and shear stresses are highly localized near the joint ends. Moreover, the interfacial normal stress is tensile and singular. This explains why the $[0/90/0/90]_{2s}$ single-lap joint suffered cohesive failure and why matrix cracks initiate from both ends of the $[90/0/90/0]_{2s}$ single-lap joint.

For the wavy-lap joint, the interfacial stress distributions are totally different from those of the flat single-lap joint. The most distinct feature is that the interfacial normal stress at the joint end is compressive. Although in the central region of the joint there are tensile interfacial normal stresses, they are relatively low and are distributed more evenly. From Fig. 12, note that most of the shear load is transferred through the middle part of the joint. This is another improvement over the flat single-lap joint.

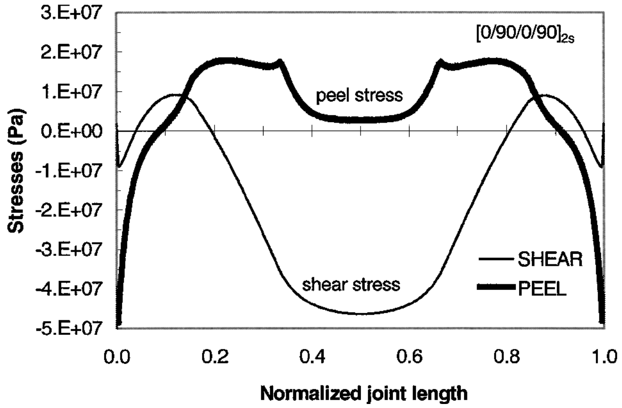

a) $[0/90/0/90]_{2s}$

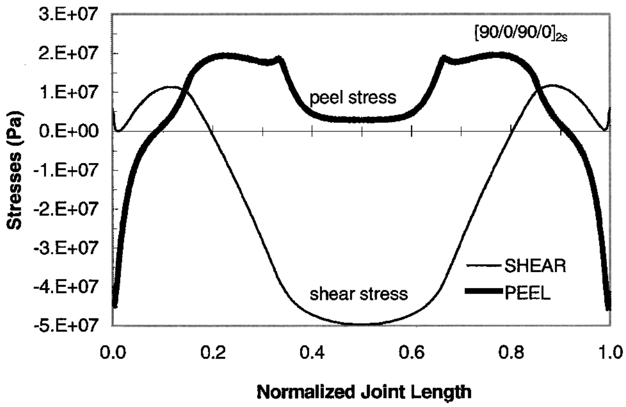

b) $[90/0/90/0]_{2s}$

Fig. 12 Interfacial stress distributions in wavy-lap joints at a tensile load of 12 kN.

Analysis of Failure Modes

Failure modes of conventional single-lap joint have been very well characterized by many researchers and will not be reiterated.[1] To provide reasonable explanations for failure modes in the new wavy joint, finite element analyses (FEA) that account for the adhesive plasticity are performed. The FEA model uses a global–local scheme, in which the global model covers the whole joint, whereas the local model is confined near the joining region where a fine mesh is used.[9]

Most polymeric materials, such as the FM73M adhesive used here, are highly nonlinear. They may also exhibit different yield stresses in tension and compression.[10] The shear stress–strain curve of the FM73M film adhesive at room temperature (24°C) provided by the manufacturer is shown in Fig. 13. By assuming the film adhesive as a J_2 elastic–plastic material, the effective stress–effective plastic strain curve can be derived from the shear stress–strain curve in Fig. 13. With this and the elastic moduli given in Table 2, the uniaxial stress–strain curve for the adhesive is obtained and used in the FEA with the ABAQUS code to analyze the interfacial stresses of the joints. Figure 14 shows the comparison of interfacial stresses obtained from the elastic and elastic–plastic analyses for the $[90/0/90/0]_{2s}$ wavy-lap joint. It is evident that the differences are very small. Thus, comparison of the elastic interfacial stresses in the foregoing section is valid.

The maximum stress failure criterion is employed for the failure analysis of the AS4/3501-6 composite adherends. The tensile and compressive strengths along and perpendicular to the fiber direction are $X_t = 2280$ MPa and $X_c = -1440$ MPa and $Y_t = 57$ MPa and $Y_c = -228$ MPa, respectively. The shear strength in the 1–2 plane is $S = 71$ MPa (Ref. 11). Failure of the composite material is indicated by the parameter defined as $\mathrm{MSTRS} = \max(\sigma_{11}/X, \sigma_{22}/Y, |\sigma_{12}/S|)$. If $\sigma_{11} > 0$, then $X = X_t$ is selected; otherwise, $X = X_c$. Similarly, if $\sigma_{22} > 0$, $Y = Y_t$; otherwise, $Y = Y_c$. The composite fails if MSTRS ≥ 1.0. The applied load is the average failure load of each respective joint.

For the wavy-lap joints with the two laminate adherends, failure was observed to initiate in the composite adherends but at different locations. Contours of MSTRS, which are not shown here, predict the failure initiation sites observed in Figs. 7 and 9. Specifically, for the $[0/90/0/90]_{2s}$ wavy-lap joint, matrix cracking occurred in the lamina that consisted of two 90-deg plies. The maximum value of MSTRS shown in Fig. 15 seems to coincide with the observed failure location. Note that the maximum value of MSTRS is greater than 1, indicating failure under the applied load.

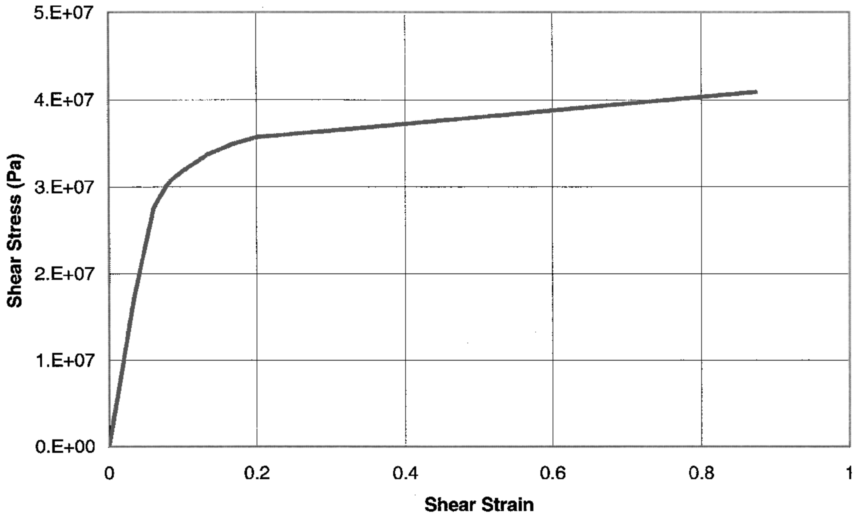

Fig. 13 Shear stress-strain curve of the FM73M film adhesive at room temperature (24°C).

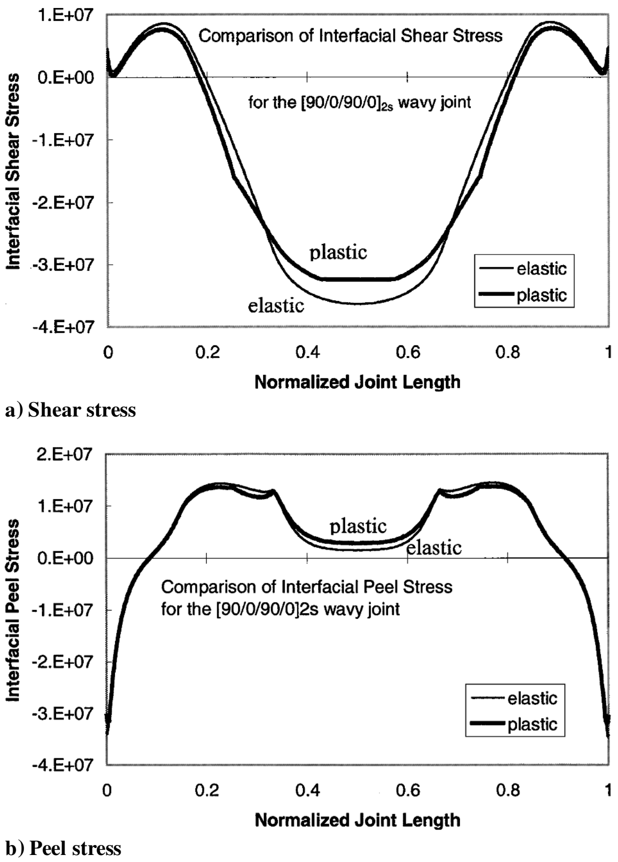

Fig. 14 Interfacial stress comparison of elastic and elastic–plastic analyses for the $[90/0/90/0]_{2s}$ wavy joint at the tensile failure load of 8.65 kN.

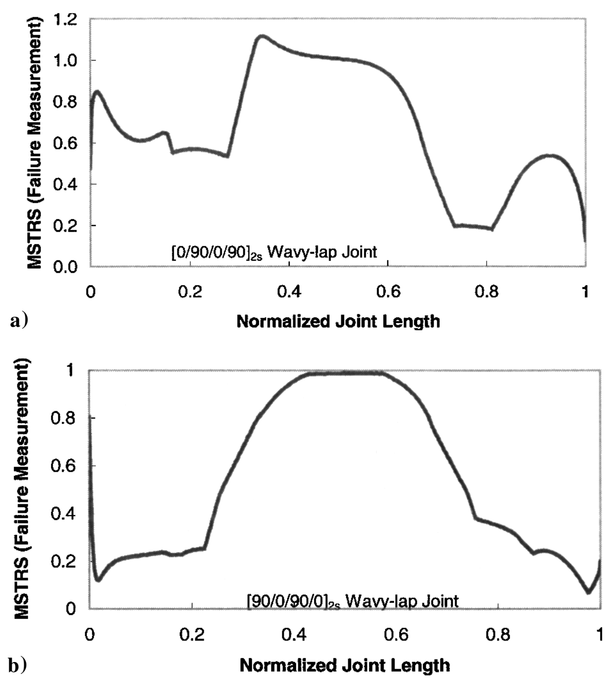

Fig. 15 Distribution of MSTRS value in the wavy-lap joint a) in the lamina that consists of two 90-deg plies in the $[0/90/0/90]_{2s}$ laminate adherend and b) in the 90-deg lamina adjacent to the adhesive in the $[90/0/90/0]_{2s}$ laminate adherend.

For the wavy-lap joint with $[90/0/90/0]_{2s}$ adherends, the maximum MSTRS value occurs in the 90-deg lamina adjacent to the adhesive layer. The distribution of MSTRS in this lamina is shown in Fig. 15. The maximum value is equal to 1 and occurs in a region that is approximately the same as the failure site indicated by Fig. 7.

Summary

It has been demonstrated that the new wavy-lap joint is much stronger than the conventional single-lap joint. From the experiments and analyses, the following conclusions have been obtained.

1) The new wavy joint design can provide a joint strength several times that of the conventional single-lap joint. This increase in joint strength depends on the stacking sequence of the composite laminate adherend.

2) In contrast to the conventional single-lap joint, which suffers singular tensile peel stress at both joint ends, the interfacial normal stress in the new wavy-lap joint is compressive near the joint ends.

3) Even though there are positive interfacial normal stresses in the central portion of the wavy-lap joint, the values are relatively small and would not initiate failure.

4) In contrast to the conventional single-lap joint in which the interfacial shear stress vanishes in the central portion of the joint, relatively large interfacial shear stresses are present in the central region of the wavy-lap joint. This means that load transfer in the wavy joint is more efficient.

5) Failure in the composite adherends in the wavy joint can be predicted by the maximum stress criterion.

Acknowledgments

The authors are grateful for the support by Office of Naval Research Grant N00014-96-1-8822 and National Science Foundation Grant 9730123-EEC to Purdue University.

References

[1] Matthews, F. L., Kilty, P. F., and Godwin, E. W., "A Review of the Strength of Joints in Fibre-Reinforced Plastics: Part 2. Adhesively Bonded Joints," *Composites*, Jan. 1982, pp. 29–37.

[2] Kinloch, A. J., *Adhesion and Adhesives*, Chapman and Hall, London 1987.

[3] Vinson, J. R., "Adhesive Bonding of Polymer Composites," *Polymer Engineering and Science*, Vol. 29, No. 19, 1989, pp. 1325–1331.

[4] Hart-Smith, L. J., "Adhesive Bonded Single Lap Joints," NASA CR-112236, Jan. 1973.

[5] Adams, R. D., "Strength Predictions for Lap Joints, Especially with Composite Adherends: A Review," *Journal of Adhesion*, Vol. 30, No. 1–4, 1989, pp. 219–242.

[6] Tsai, M. Y., and Morton, J., "The Effect of a Spew Fillet on Adhesive Stress Distributions in Laminated Composite Single-Lap Joints," *Composite Structures*, Vol. 32, No. 1–4, 1995, pp.123–131.

[7] Carpenter, W. C., "A Comparison of Numerous Lap Joint Theories for Adhesively Bonded Joints," *Journal of Adhesion*, Vol. 35, No. 1, 1991, pp. 55–73.

[8] Tsai, M. Y., Oplinger, D. W., and Morton, J., "Improved Theoretical Solutions for Adhesive Lap Joints," *International Journal of Solids and Structures*, Vol. 35, No. 12, 1998, pp. 1163–1185.

[9] ABAQUS/Standard User's Manual, Ver. 5.7, Hibbitt, Karlsson, and Sorensen, Inc., Pawtucket, RI, 1997.

[10] Raghava, R., Caddel, R. M., and Yeh, G. S., "The Macroscopic Yield Behavior of Polymers," *Journal of Materials Science*, Vol. 8, No. 2, 1973, pp. 225–232.

[11] Daniel, I. M., and Ishai, O., *Engineering Mechanics of Composite Materials*, Oxford Univ. Press, Oxford, 1994.

A. M. Waas
Associate Editor